Electronic Supplementary Information

Moisture induced isotopic carbon dioxide trapping from ambient air

Sankar Das, Chiranjit Ghosh and Subhra Jana*

Department of Chemical, Biological & Macro-Molecular Sciences, S. N. Bose National Centre for Basic Sciences, Block - JD, Sector-III, Salt Lake, Kolkata -700098, India.
E-mail: subhra.jana@bose.res.in

Contents **Page no.**

Materials. For the synthesis of adsorbents, N-[3-(trimethoxysilyl)propyl]ethylenediamine and N^1-(3-trimethoxysilylpropyl)diethylenetriamine and halloysite nanotubes (HNTs) were obtained from Sigma-Aldrich. (3-aminopropyl)triethoxysilane was purchased from Alfa Aesar. Toluene and ethanol were received from Merck.

Table S1 List of aminosilanes for the synthesis of adsorbents.

Aminosilanes	**Structure**
(3-aminopropyl)trimethoxysilane	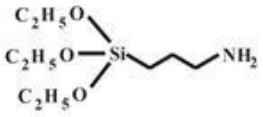
N-[3-(trimethoxysilyl)propyl] ethylenediamine	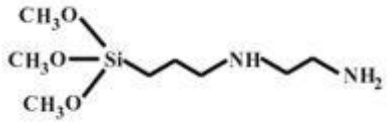
N1-(3-trimethoxysilylpropyl) diethylenetriamine	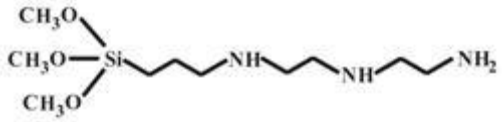

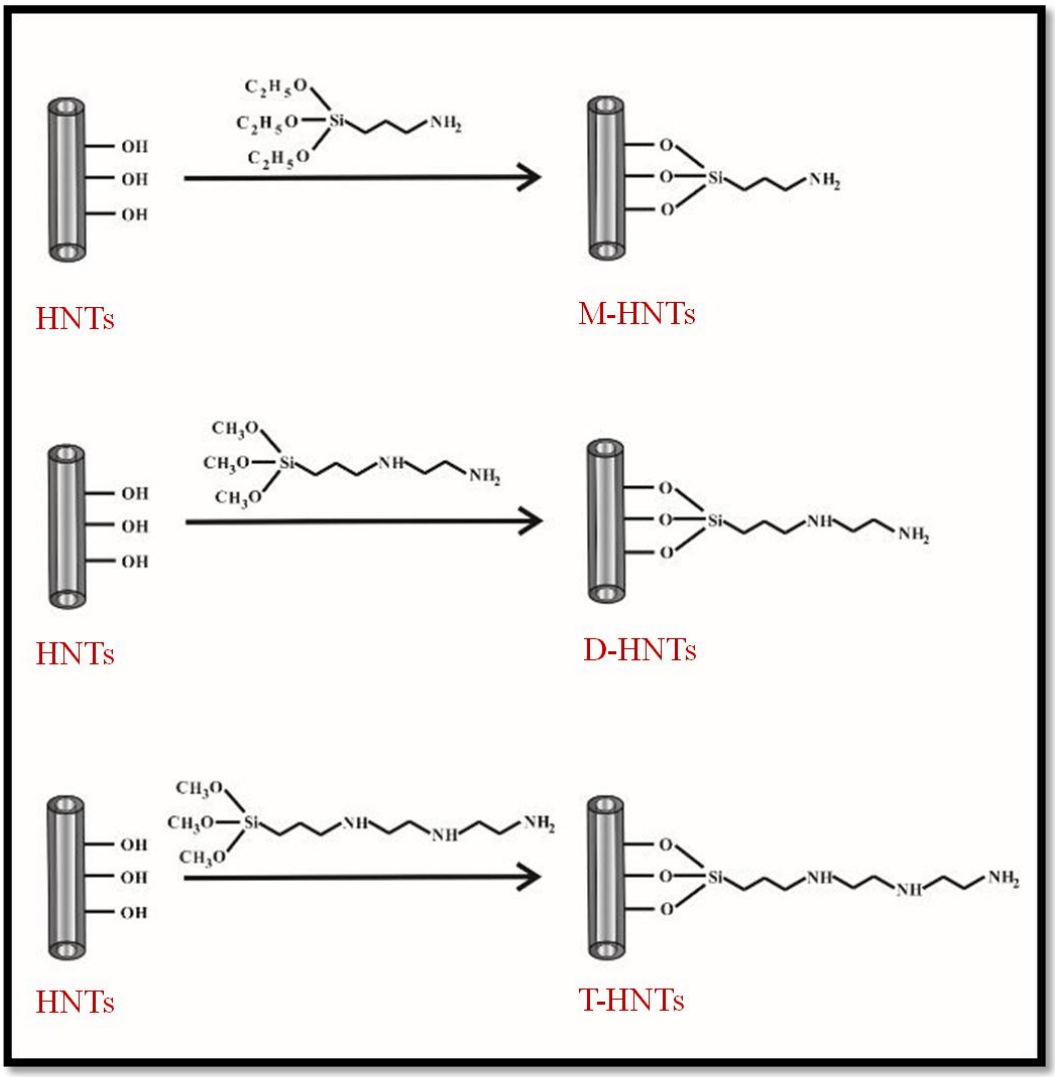

Fig. S1 Schematic presentation of the synthesis of clay based adsorbents through the immobilization of (3-aminopropyl)trimethoxysilane, N-[3-(trimethoxysilyl)propyl] ethylenediamine and N1-(3-trimethoxysilylpropyl)diethylenetriamine respectively over the surface of HNTs based on the grafting reaction to achieve M-HNTs, D-HNTs and T-HNTs.

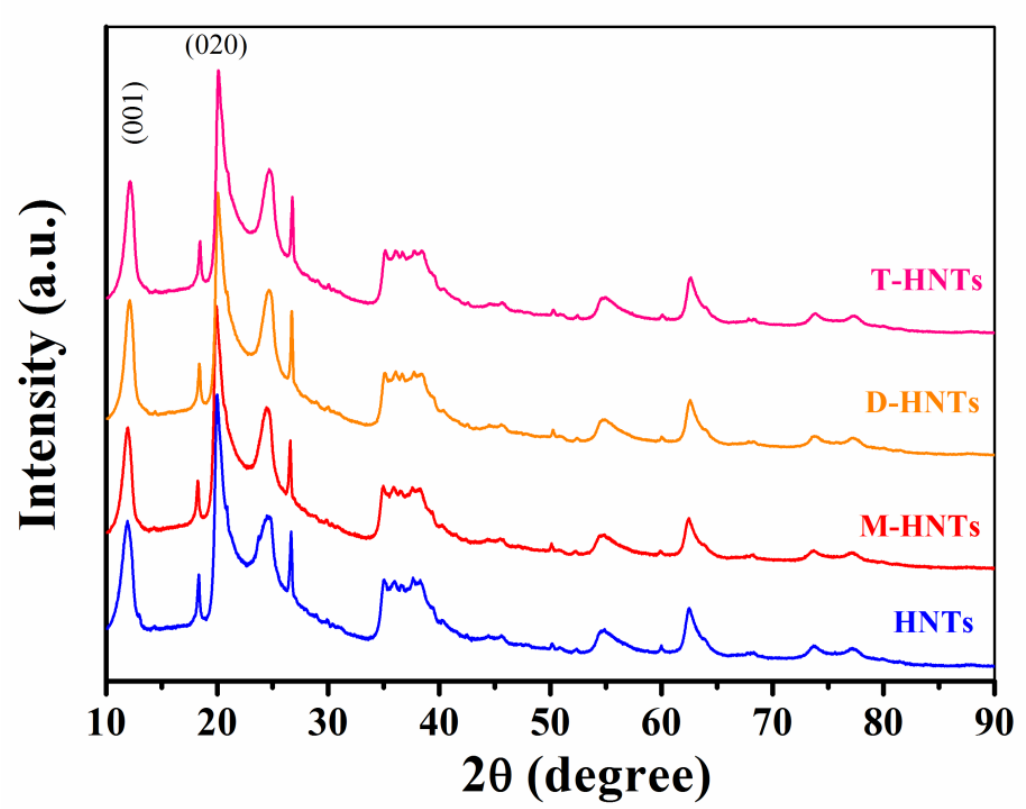

Fig. S2 XRD patterns of bare HNTs and as-prepared adsorbents, M-HNTs, D-HNTs and T-HNTs obtained through the surface modification of bare HNTs using three viable amines; (3-aminopropyl) triethoxysilane (M-HNTs), N-[3-(trimethoxysilyl)propyl]ethylenediamine (D-HNTs), and N^1-(3-trimethoxysilylpropyl) diethylenetriamine (T-HNTs) respectively.

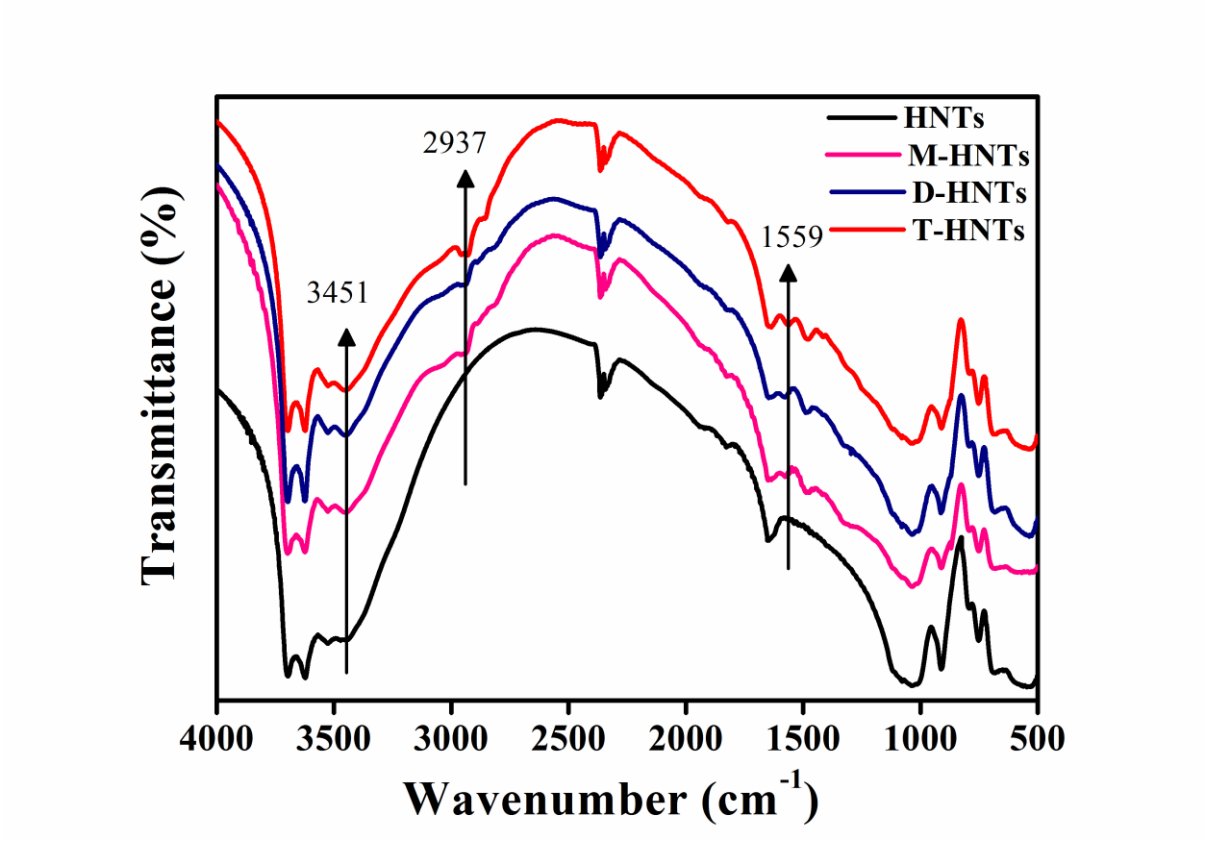

Fig. S3 FTIR spectra of M-HNTs, D-HNTs and T-HNTs demonstrate the presence of amino group in the adsorbents due to the grafting of aminosilanes onto the surface of HNTs. All FTIR spectra were recorded in the transmission mode using KBr technique. Throughout the analysis, the number of scan was fixed to 50 with a resolution of 2 cm^{-1}.

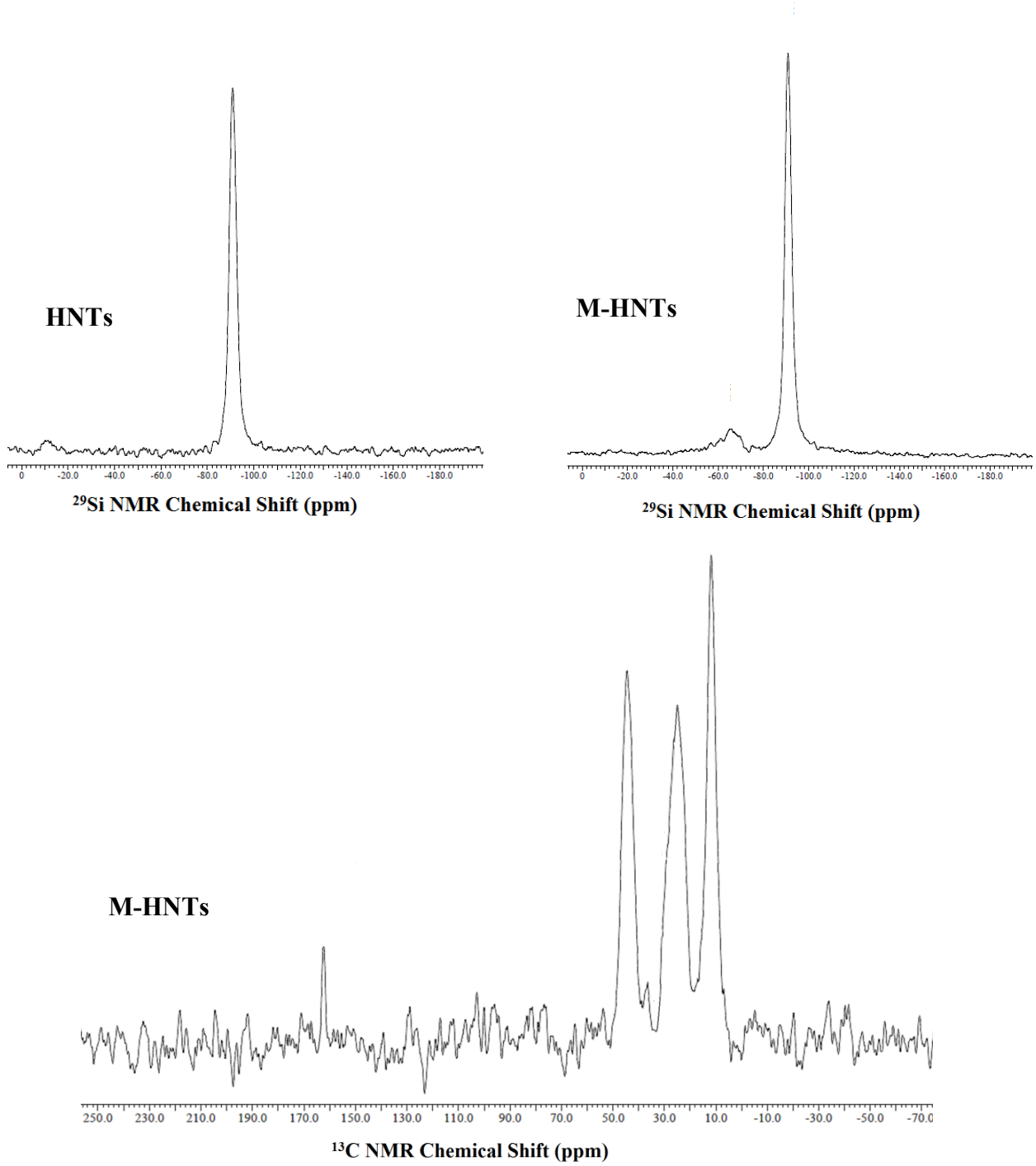

Fig. S4 ^{29}Si and ^{13}C CP-MAS NMR spectra of HNTs and M-HNTs respectively, recorded using a JEOL JNM-ECX400II spectrometer. The chemical shift at – 91 ppm arises due to presence of silicon in both HNTs and M-HNTs. The new peak at – 67 ppm in M-HNTs is assigned to the tridentate (T^3) bonded silicon, indicating the hydrolysis of all the three ethoxy groups of (3-aminopropyl)triethoxysilane, which further demonstrates the formation of new chemical bond between the surface hydroxyl groups of HNTs and the organosilane.[1,2] The chemical shifts at 11.8, 24.9 and 44.4 ppm in ^{13}C CP-MAS NMR spectrum of M-HNTs represent the three carbons in the propyl chain of the aforesaid grafted organosilane over the surface of HNTs to form M-HNTs.

Table S2 Elemental composition of the adsorbents from CHN elemental analysis.

Adsorbents	C (%)	H (%)	N (%)
M-HNTs	1.81	1.63	0.51
D-HNTs	2.73	1.96	1.05
T-HNTs	3.71	2.25	1.6

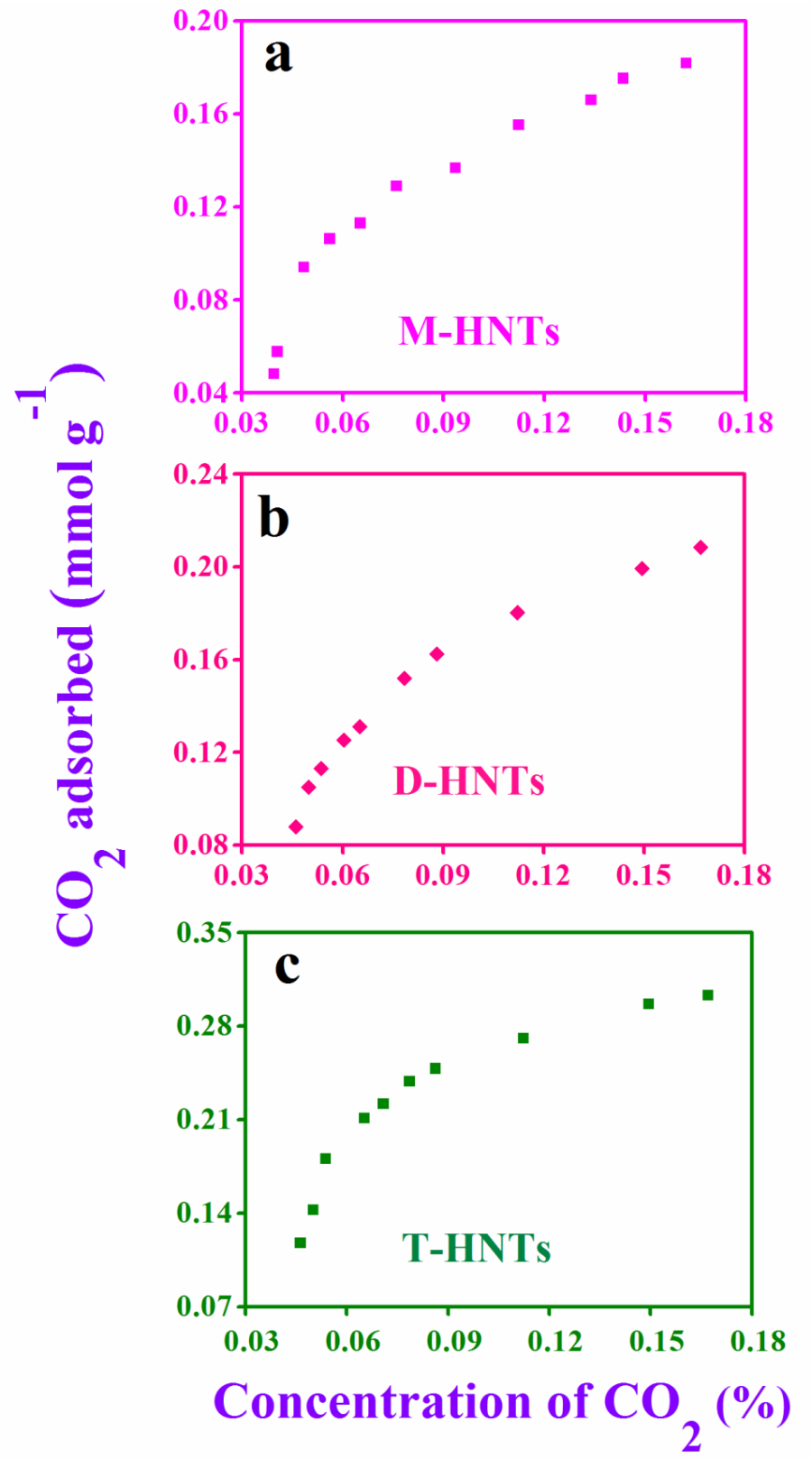

Fig. S5 CO_2 adsorption capacity of M-HNTs, D-HNTs and T-HNTs at different CO_2 concentration, demonstrating the adsorption efficacy of the adsorbents depends on the feed gas concentration.

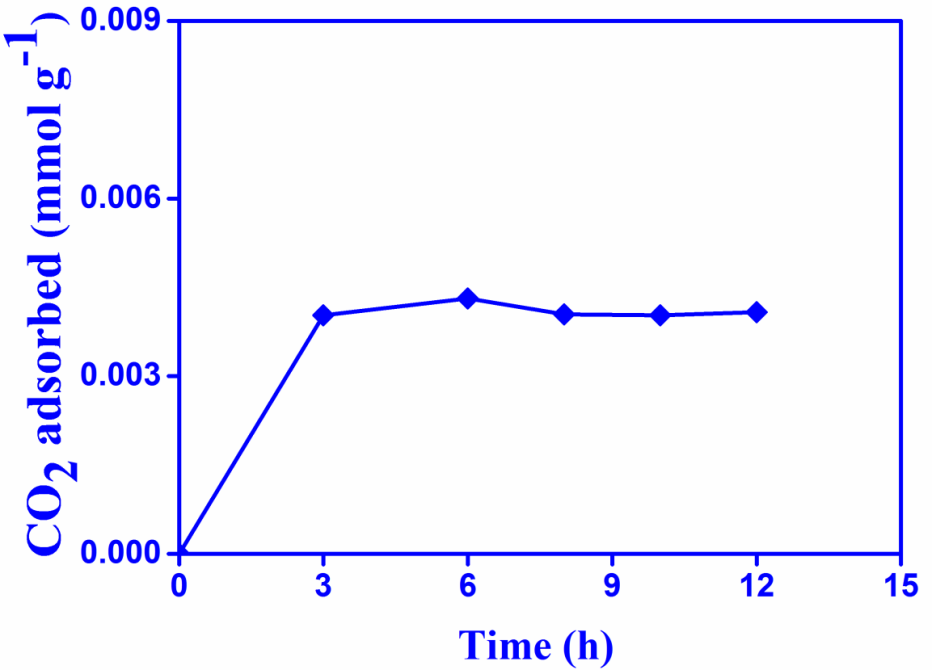

Fig. S6 Ambient CO_2 adsorption by bare HNTs at standard pressure and temperature measured using OA-ICOS, demonstrating that they hardly possess any adsorption efficiency.

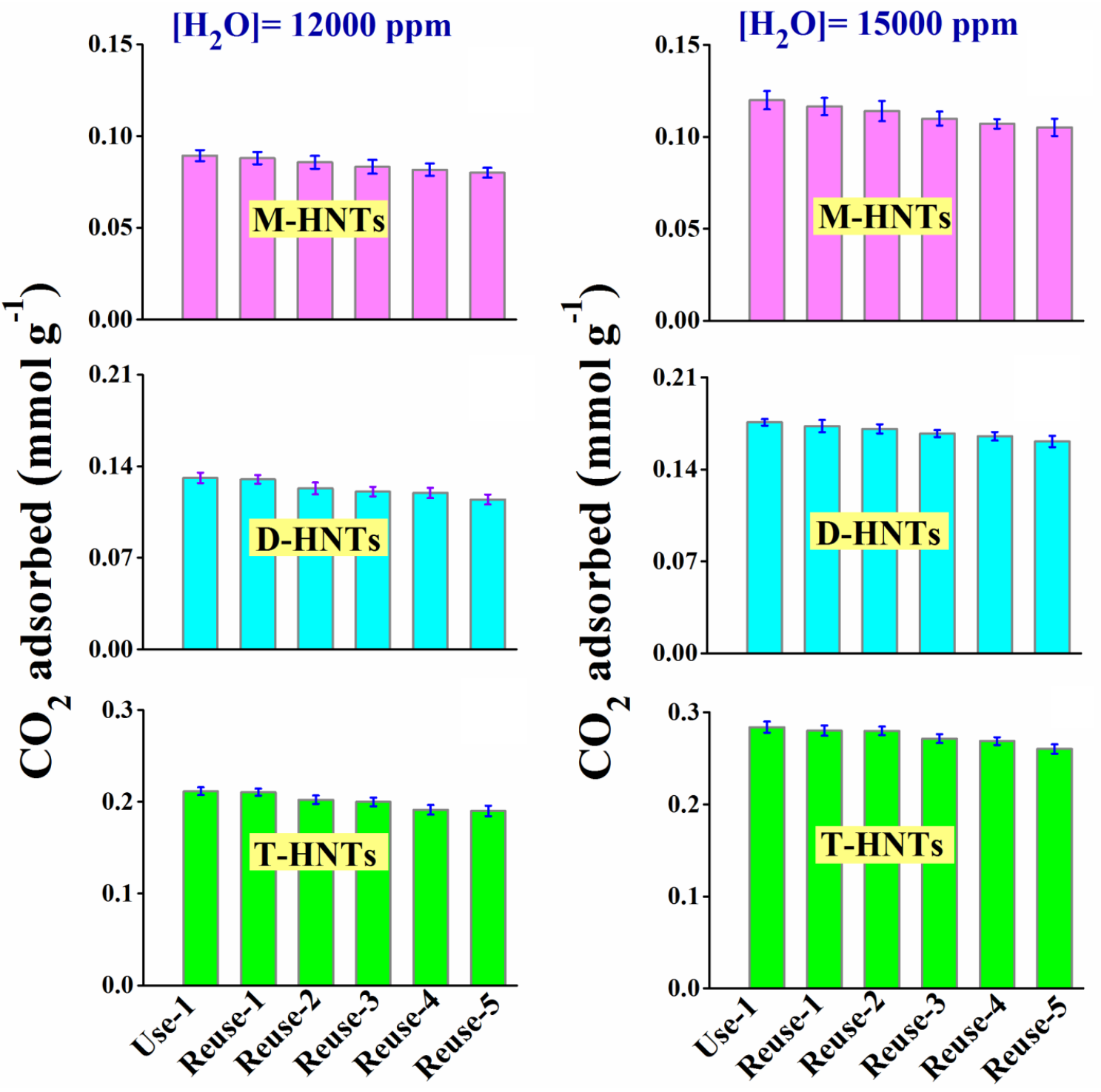

Fig. S7 The regeneration and recyclability of M-HNTs, D-HNTs, and T-HNTs adsorbents for atmospheric CO_2 capture at different moisture concentration, signifying the good thermal stability and reusability of all adsorbents even under oxidative environment.

Table S3 Comparison of CO_2 uptake efficacy of these clay based adsorbents with the reported amine based solid adsorbents.

Adsorbents	Feed gas concentration [CO_2] in vol %	Amine loading ($mmol_N\ g^{-1}$)	Amine efficiency ($mmol_{CO2}\ mmol_N^{-1}$)	References
$APTES_{39}$/MCM	100	1.79	0.26	3
A2-SBA-15	100	4.20	0.34	4
A2-BPMO	100	4.90	0.44	4
DWSNT-NH_2	100	2.93	0.49	5
DWSNT-NH-$(CH_2)_2$-NH_2	100	4.57	0.41	5
DWSNT-NH-$(CH_2)_2$-NH-$(CH_2)_2$-NH_2	100	4.93	0.45	5
APS-MCM-48	100	2.45	0.32	6
NH_2-mag[a]	100	2.20	0.16	7
NH_2-C_{18}-mag[a]	100	2.30	0.52	7
APS/SBA(1)	15.4	1.11	0.14	8
AEAPS/SBA(1)	15.4	2.26	0.12	8
TA/SBA(1)	15.4	2.75	0.13	8
SBA-NH_2	10	1.90	0.21	9
SBA-diamine	10	2.50	0.28	9
APTMS/SBA-ex	10	2.43	0.44	10
AEAPS/SBA-ex	10	3.41	0.29	10
TA/SBA-ex	10	4.76	0.25	10
AMPTS/Magnesium Phyllosilicate[b]	5	2.56	0.89	11
TMSPEDA/Magnesium Phyllosilicate[b]	5	3.37	0.84	11
TMSPETA/Magnesium Phyllosilicate[b]	5	3.24	0.71	11
HYB-maga28[c]	5	0.220	0.60	12

γ-maga28	5	0.276	0.37	12
M-HNTs	0.04	0.36	0.36	present work
D-HNTs	0.04	0.75	0.25	present work
T-HNTs	0.04	1.14	0.25	present work

a: Relative humidity of the gas stream is ~74%. The presence of octadecyl groups in NH_2-C_{18}-mag expanded the interlayer space and help to increase CO_2 adsorption capacity; ***b***: Besides alkylammonium carbamate other compounds, like silylpropylcarbamates and hydrogen-bonded propylcarbamic acids were formed, increasing the efficiency above 0.5; ***c***: HYB-maga28 is a pillared layered silicates, where lamellas are separated by pillars, allowing CO_2 to reach to amine site and also the surface SiOH groups also take part in the adsorption process by forming silylpropylcarbamates, hydrogen-bonded propylcarbamic acids etc, increasing the efficiency beyond 0.5.

APTES: 3-aminopropyltriethoxysilane; A2-SBA-15: N-[3-(trimethoxysilyl)propyl]ethylene-diamine modified SBA-15; A2-BPMO: N-[3-(trimethoxysilyl) propyl]-ethylenediamine-modified benzene periodic mesoporous organosilica; DWSNTs: double-walled silica nanotubes; APS: 3-aminopropyltriethoxysilane; NH_2-mag: 3-aminopropyltriethoxysilane modified magadiite; NH_2-C_{18}-mag: 3-aminopropyltriethoxysilane and octadecyltrichlorosilane modified magadiite; AEAPS: N-(2-aminoethyl)-3-aminopropyltrimethoxysilane; TA: (3-trimethoxysilylpropyl)diethylenetriamine; SBA-NH_2: 3-amino-propyltriethoxysilane functionalized SBA silica; SBA-diamine: N-[3-(trimethoxysilyl)propyl] ethylenediamine functionalized aminosilicas; AMPTS: 3-aminopropyltriethoxysilane; TMSPEDA: N-[3-(trimethoxysilyl)propyl]-ethylenediamine; TMSPETA: N-[3-(trimethoxysilyl)propyl]-diethylenetriamine; **γ**-maga28: γ-aminopropyltriethoxysilane functionalized magadiite; HYB-maga28: γ-aminopropyltriethoxysilane functionalized magadiite i.e.; pillared layered silicates.

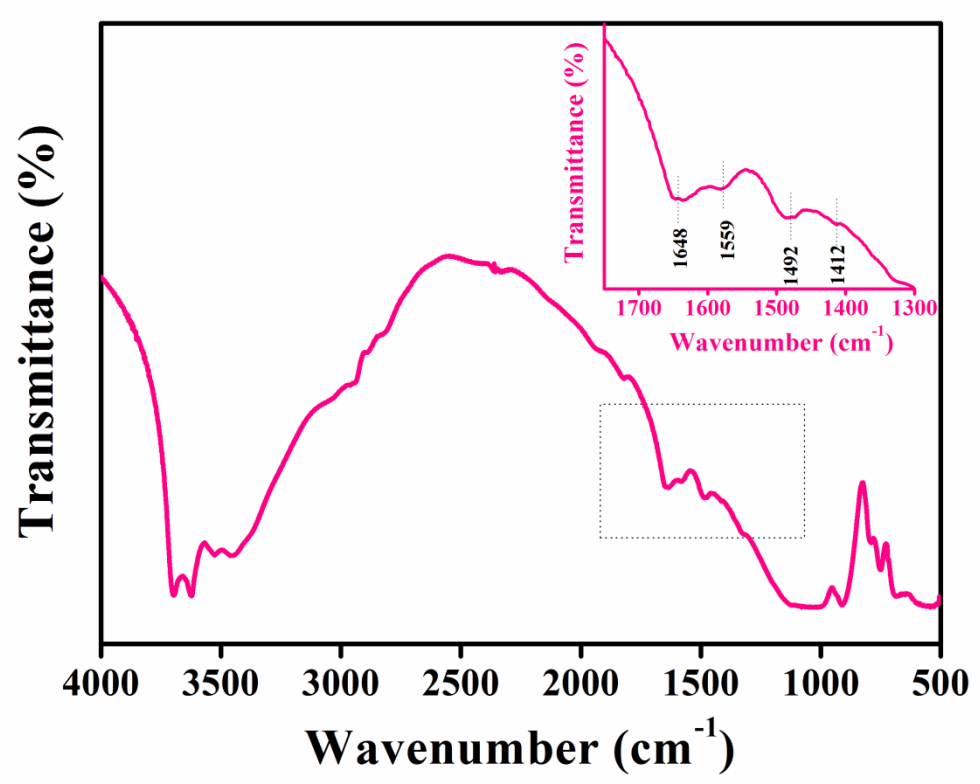

Fig. S8 FTIR spectrum after the adsorption of CO_2 on T-HNTs demonstrates the formation of alkylammonium carbamate species owing to the adsorption of atmospheric CO_2 onto the surface of the adsorbent.

Table S4 Assignment of FTIR bands after the adsorption of atmospheric CO_2 over the surface of adsorbent.

Wavenumber (cm^{-1})	**Assignment**	**Species**	**References**
1412	Symmetric stretching COO-	Carbamate	13,14, 15
1492	Symmetric NH^+ deformation	Ionic carbamate	3,14,15
1559	N-H deformation	Aminosilane	1
1648	C=O stretching	Carbamic acid	16, 17
2937	C–H stretching vibration	Aminosilane	1, 18
3451	N–H stretching vibration	Aminosilane	1

References

1 P. Yuan, P. D. Southon, Z. Liu, M. E. R. Green, J. M. Hook, S. J. Antill and C. J. Kepert, *J. Phys. Chem. C*, 2008, **112**, 15742-15751.

2 S. A. Didas, A. R. Kulkarni, D. S. Sholl and C. W. Jones, *ChemSusChem*, 2012, **5**, 2058−2064.

3 U. Tumuluri, M. Isenberg, C. Tan and S. S. C. Chuang, *Langmuir*, 2014, **30**, 7405−7413.

4 K. Sim, N. Lee, J. Kim, E. B. Cho, C. Gunathilake and M. Jaroniec, *ACS Appl. Mater. Interfaces*, 2015, **7**, 6792−6802.

5 Y.G. Ko, H. J. Lee, H.C. Oh and U. S. Choi, *J. Hazard. Mater*., 2013, **53**, 250-251.

6 S. Kim, J. Ida, V. V. Guliants and J. Y. S. Lin, *J. Phys. Chem. B*, 2005, **109**, 6287−6293.

7 Y. Ide, N. Kagawa, M. Sadakane and T. Sano, *Chem. Commun*., 2013, **49**, 9027−9029.

8 N. Hiyoshi, K. Yogo and T. Yashima, *Microporous Mesoporous Mater*., 2005, **84**, 357–365.

9 J. C. Hicks, J. H. Drese, D. J. Fauth, M. L. Gray, G. Qi and C. W. Jones, *J. Am. Chem. Soc*., 2008, **130**, 2902-2903.

10 Y. Li, N. Sun, L. Li, N. Zhao, F. Xiao, W. Wei, Y. Sun and W. Huang, *Material*s, 2013, **6**, 981−999.

11 K. O. Moura and H. O. Pastore, *Environ. Sci. Technol*., 2013, **47**, 12201−12210.

12 H. M. Moura and H. O. Pastore, *Dalton Trans*., 2014, **43**, 10471–10483.

13 W. C. Wilfong, C. S. Srikanth and S. S. C. Chuang, *ACS Appl. Mater. Interfaces*, 2014, **6**, 13617−13626.

14 M. W. Hahn, M. Steib, A. Jentys and J. A. Lercher, *J. Phys. Chem. C*, 2015, **119**, 4126−4135.

15 M. J. Al-Marri, M. M. Khader, M. Tawfik, G. Qi, E. P. Giannelis, *Langmuir*, 2015, **31**, 3569−3576.

16 C. Knöfel, C. Martin, V. Hornebecq and P. L. Llewellyn, *J. Phys. Chem. C*, 2009, **113**, 21726–21734.

17 Z. Bacsik, N. Ahlsten, A. Ziadi, G. Zhao, A. E. Garcia-Bennett, B. Martín-Matute and N. Hedin, *Langmuir*, 2011, **27**, 11118–11128.

18 A. Zhao, A. Samanta, P. Sarkar and R. Gupta, *Ind. Eng. Chem. Res.*, 2013, **52**, 6480−6491.